Enhanced subunit interactions with gemcitabine-5′-diphosphate inhibit ribonucleotide reductases

Jun Wang[†], Gregory J. S. Lohman[†‡], and JoAnne Stubbe[†§¶]

Departments of [†]Chemistry and [§]Biology, Massachusetts Institute of Technology, Cambridge, MA 02139

Contributed by JoAnne Stubbe, July 23, 2007 (sent for review June 20, 2007)

Ribonucleotide reductases (RNRs) catalyze the conversion of nucleotides to deoxynucleotides in all organisms. The class I RNRs are composed of two subunits, α and β, with proposed quaternary structures of $\alpha2\beta2$, $\alpha6\beta2$, or $\alpha6\beta6$, depending on the organism. The α subunits bind the nucleoside diphosphate substrates and the dNTP/ATP allosteric effectors that govern specificity and turnover. The $\beta2$ subunit houses the diferric $Y^{\bullet}$ (1 radical per $\beta2$) cofactor that is required to initiate nucleotide reduction. 2′,2′-Difluoro-2′-deoxycytidine (F_2C) is presently used clinically in a variety of cancer treatments and the 5′-diphosphorylated F_2C (F_2CDP) is a potent inhibitor of RNRs. The studies with [1′-^{3}H]-F_2CDP and [5-^{3}H]-F_2CDP have established that F_2CDP is a substoichiometric mechanism based inhibitor (0.5 eq F_2CDP/α) of both the *Escherichia coli* and the human RNRs in the presence of reductant. Inactivation is caused by covalent labeling of RNR by the sugar of F_2CDP (0.5 eq/α) and is accompanied by release of 0.5 eq cytosine/α. Inactivation also results in loss of 40% of $\beta2$ activity. Studies using size exclusion chromatography reveal that in the *E. coli* RNR, an $\alpha2\beta2$ tight complex is generated subsequent to enzyme inactivation by F_2CDP, whereas in the human RNR, an $\alpha6\beta6$ tight complex is generated. Isolation of these complexes establishes that the weak interactions of the subunits in the absence of nucleotides are substantially increased in the presence of F_2CDP and ATP. This information and the proposed asymmetry between the interactions of αnβn provide an explanation for complete inactivation of RNR with substoichiometric amounts of F_2CDP.

Gemcitabine, or 2′,2′-difluoro-2′-deoxycytidine (F_2C), is a drug that is used clinically in the treatment of advanced pancreatic cancer and non-small cell lung carcinomas (1–3). In humans, F_2C enters the cell via CNT-type or ENT-type transporters (4–6) and must be phosphorylated to exhibit its cytotoxicity. The monophosphate of F_2C (F_2CMP) is generated by deoxycytidine kinase (7) and is rapidly phosphorylated to the di- and triphosphates (F_2CDP and F_2CTP) (8, 9). Diphosphorylated F_2C (F_2CDP) is an irreversible inhibitor of ribonucleotide reductase (RNR) (10–13), and F_2CTP functions as a chain terminator in the DNA polymerase reaction (14, 15). Differentially phosphorylated states of gemzar can also interfere with other enzymes involved in nucleotide metabolism. The mechanisms of cytotoxicity of F_2C depend on the phosphorylated state of the inhibitor and are likely to be cell specific and multifactoral. Our recent synthesis of [1′-^{3}H]-F_2CDP has provided the required tool to investigate the mechanism by which this molecule inactivates RNRs. Studies reported herein provide a previously unrecognized approach for RNR inhibition, one in which the mechanism based inhibitor (F_2CDP) enhances the interactions between the two subunits of RNR preventing nucleotide reduction despite substoichiometric labeling.

RNRs catalyze the conversion on nucleoside di(tri)phosphates to deoxynucleoside di(tri)phosphates in all organisms and are the predominant control point for abundance and ratios of dNTPs pools required for the initiation and elongation processes catalyzed by DNA polymerases (16, 17). The class I RNRs are composed of two types of subunits, α and β. The quaternary structure of α is nucleotide- and organism-dependent. It can be a monomer, dimer, tetramer, or hexamer (16, 18). β is a homodimer that houses the diferric-tyrosyl radical ($Y^{\bullet}$) required for initiating nucleotide reduction on α. Current evidence suggests that there is one $Y^{\bullet}$ and 2 di-iron clusters/$\beta2$ (19, 20). The interactions between α and β are weak (K_d of 0.2 μM) in the absence of nucleotide (21). In prokaryotic systems α and β are both homodimers. The active *Escherichia coli* RNR is thought to be an $\alpha2\beta2$ complex (22, 23). The α oligomeric state of the mouse RNR has been the best characterized eukaryotic RNR to date. In the absence of nucleotides, α is a monomer. It dimerizes in the presence of allosteric effectors (dATP, TTP, dGTP, and ATP) (18). In addition, the millimolar levels of ATP found intracellularly cause α to oligomerize to a hexamer ($\alpha6$). β is a homodimer ($\beta2$). The quaternary structure of eukaryotic RNRs is still being actively investigated. The complex responsible for RNR activity has been proposed by Cooperman and coworkers (18) to be $\alpha2\beta2$, $\alpha6\beta2$, or $\alpha6\beta6$ on the basis of a variety of physical biochemical and kinetic studies. Recent gas-phase electrophoretic-mobility macromolecule analysis studies have suggested that the mouse quaternary structure is $\alpha6\beta2$ (24). Studying subunit interactions has been difficult by conventional methods because of α's nucleotide-dependent aggregation state and the weak binding of α and β, which is also nucleotide-dependent (21). Determination of apparent molecular masses of the active RNR complexes requires nucleotides in the analysis buffer, and thus protein detection by UV spectroscopy is obscured (18, 23).

A number of years ago, we reported on the inactivation of *E. coli* RNR by F_2CDP (11, 12). We showed that 1 eq of F_2CDP per *E. coli* RNR, presumably $\alpha_2\beta_2$, in the presence of reductants, thioredoxin (TR) and TR reductase or DTT, is sufficient for enzyme inactivation and that the inactivation is accompanied by release of 2 fluoride ions and one cytosine (12). We also demonstrated that the mode of inhibition changed in the absence of reductants. Thus, as with all nucleotide mechanism based inhibitors of RNRs studied in detail, multiple modes of inactivation are involved in the inhibition process (Scheme 1). The details of the inhibition by F_2CDP have remained largely unexplored because of the unavailability of sugar and base radiolabeled F_2CDP. We have recently developed a method to synthesize [1′-^{3}H]-F_2CDP and [5-^{3}H]-F_2CDP (9). These compounds have allowed us to reinvestigate the mechanism of inhibition of the *E. coli* RNR and to report for the first time on the details of the inhibition of the human RNR. The present communication shows that incubation of human and *E. coli* RNRs with [1′-^{3}H] or [5-^{3}H] F_2CDP results in 1 eq of sugar covalently bound per α_2, which is sufficient for RNR inactivation. Size exclusion chromatography (SEC) of the inactivated RNRs reveals that this modification of α dramatically alters αn/βn subunit interactions,

Author contributions: J.S. designed research; J.W. and G.J.S.L. performed research; J.W., G.J.S.L., and J.S. analyzed data; and J.S. wrote the paper.

The authors declare no conflict of interest.

Abbreviations: F_2C, 2′,2′-difluoro-2′-deoxycytidine; F_2CDP, diphosphorylated F_2C; RNR, ribonucleotide reductase; TR, thioredoxin; SEC, size exclusion chromatography.

[‡]Present address: Momenta Pharmaceuticals, 675 West Kendall Street, Cambridge, MA 02142.

[¶]To whom correspondence should be addressed. E-mail: stubbe@mit.edu.

This article contains supporting information online at www.pnas.org/cgi/content/full/0706803104/DC1.

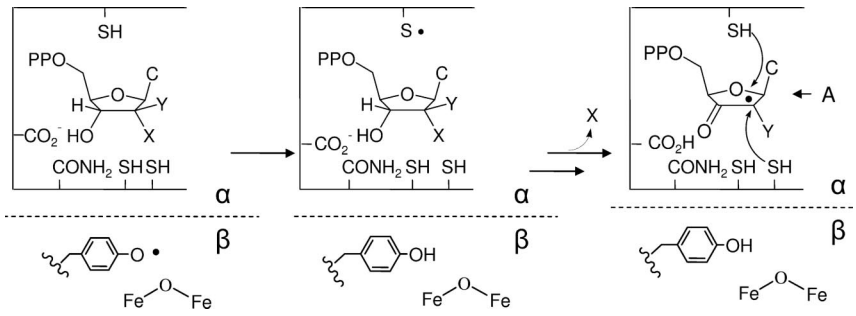

Scheme 1.

forming a tight complex, which is ultimately responsible for complete RNR inhibition.

Results

Synthesis of [1′-^{3}H]-F_2CDP and [5-^{3}H]-F_2CDP. Synthesis of [1′-^{3}H]-F_2C involved modification of previously published procedures (25, 26). The 2-deoxy-3,5-di-*O*-benzoyl-3,3-difluororibonolactone was reduced with [^{3}H]-disiamylborane made from NaB^3H_4 and 2-methyl-2-butene. The lactol formed was converted without purification to 2-deoxy-3,5-di-*O*-benzoyl-3,3-difluoro-1-*O*-methanesulfonyl-D-ribofuranoside which was then coupled with bis(trimethylsilyl)-cytosine to give, subsequent to deblocking, an α,β mixture (60:40) of [1′-^{3}H]-F_2C. Phosphorylation to the monophosphate (F_2CMP) was effected by using human deoxycytidine kinase (7). Because only the β isomer of the nucleoside is a substrate, this step allowed removal of α F_2C. F_2CMP was then phosphorylated to the diphosphate with human UMP/CMP kinase (8). The details of this syntheses will be reported elsewhere (9).

Purification of the α and β Subunits of Human RNR. The clones for α and β were obtained from the Y. Yen laboratory (City of Hope National Medical Center, Duarte, CA). Mutations in the genes were corrected to the sequence reported in the National Center for Biotechnology Information (NCBI) database (27, 28), and the N terminus of each protein was reengineered to maintain the $(His)_6$ tag and to reduce the length of the intervening linker before the start of the gene to 10 aa. The proteins were purified to ≈90% homogeneity based on SDS/PAGE, using Ni affinity chromatography.

β2 as isolated is a dimer in the apo form and was reconstituted by following the protocol we have developed for reconstitution of the *E. coli* β2 (29). The resulting protein had 0.8 tyrosyl radicals/β2 and a specific activity of 1,089 nmol/min/mg in the presence of a 7-fold excess of α. α was difficult to work with because of its low solubility. However, its specific activity in the presence of a 7-fold excess of β was 462 nmol/min/mg. These results contrast with previous reports in the literature of 75 nmol/min/mg and 158 nmol/min/mg for β and 6.8 nmol/min/mg for α (30, 31). The basis for the activity differences are not understood, but are likely related to the complexity of the assay as we articulated in detail in ref. 32.

Table 1. Covalent labeling of *E. coli* and human RNR with [1′-^{3}H]-F_2CDP and [5-^{3}H]-F_2CDP analyzed by SEC

Protein	[^{3}H]-F_2CDP	Conditions	[^{3}H]/α2
E. coli RNR	1′	Native	0.9
	1′	Denaturing	1.11
	5	Native	0.19
	5	Denaturing	0.08
Human RNR	1′	Native	0.85
	1′	Denaturing	0.8
	5	Native	0.1

Time-Dependent Inactivation of Human and *E. coli* RNRs. Our previous studies of the mechanism of F_2CDP inactivation of RNR were carried out on the *E. coli* enzyme, by using unlabeled inhibitor. Our results were provocative in that 1 mol of F_2CDP inactivated 1 mol of $\alpha2\beta2$, which has two active sites. The experiments have been repeated by using [1′-^{3}H]-F_2CDP and [5-^{3}H]-F_2CDP. Incubation of 15 μM α2 and 15 μM β2 with 15 or 30 μM of [1′-^{3}H]-F_2CDP resulted in recovery of 0.9 (1.1) mol of radiolabel/RNR ($\alpha2\beta2$) from analysis of the reaction mixture that was passed through a Sephadex G50 column in the absence or presence of denaturant (Table 1). With the [5-^{3}H]-F_2CDP, 0.19 and 0.08 eq were detected in the absence or presence of denaturant, respectively. These results establish that there is 1 eq of the sugar from F_2CDP covalently bound to the enzyme and that most of the cytosine has been released. In addition, under these conditions, 40% of the tyrosyl radical is lost similar to our previous studies (12). These results, in conjunction with the time-dependent inactivation studies, establish that substoichiometric amounts of F_2CDP completely inactivate the *E. coli* RNR.

A similar set of experiments has been carried out on the human RNR. Time-dependent inactivation studies in which the inactivation mixture contained 0.5, 1.0, or 5.0 eq of F_2CDP/α reveal that 0.5 eq of F_2CDP/α results in complete loss of RNR activity (Fig. 1). The instability of the β2 radical requires that a control in the absence of F_2CDP be carried out and used to correct the data observed in its presence. The weak interaction between α and β of RNR allow assays of the subunit activity individually (21, 32). Thus, the inactivation mixture was assayed for activity of α (β) in the presence of a 7-fold excess of β (α). Under these conditions, α is 100% inactive. In contrast to expectations, β retained 60–70% of its activity [supporting information (SI) Fig. 4], suggesting that the excess α is capable of facilitating subunit dissociation. The results of these experiments have interesting implications in recovering RNR activity *in vivo* subsequent to its inactivation by F_2CDP and will be discussed subsequently.

Studies using [1′-^{3}H]-F_2CDP and [5-^{3}H]-F_2CDP were carried out

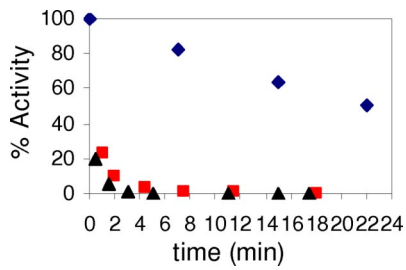

Fig. 1. Time-dependent inactivation of human RNR by F_2CDP. Inactivation mixture contained final concentrations of α, β, 1.2 μM; F_2CDP, 0.6 μM (■), and 6 μM (▲); ATP, 3 mM; and DTT, 5 mM. Aliquots were removed at various times and diluted 4-fold for determination of RNR activity. Control experiment (♦) is identical to the experiment except that F_2CDP was omitted.

to determine whether the label was attached covalently. Incubation of [1′-^{3}H] or [5-^{3}H]-F_2CDP with human RNR followed by Sephadex G50 chromatography under native and denaturing conditions gave the results summarized in Table 1. With the [1′-^{3}H] F_2CDP 0.8–0.85 labels were bound per α2, whereas with the [5-^{3}H] only 0.1 labels were covalently bound. The results are very similar to those observed with the *E. coli* RNR, with the unusual stoichiometry of 1 F_2CDP per α2 observed.

Cytosine Release by Human RNR. The inactivation studies suggested that covalent modification is accompanied by cytosine release. To test this hypothesis, 2 eq of [5-^{3}H] F_2CDPs were incubated with α2β2. Subsequent to inactivation the nucleotides were recovered by ultrafiltration and analyzed by HPLC. The analysis revealed 1 eq of cytosine and 1 eq of F_2CDP. These results parallel those reported for inactivation of *E. coli* RNR (12) and support the model that inactivation can be achieved with substoichiometric amounts of F_2CDP.

Subunit Interactions of *E. coli* RNR in the Presence of F_2CDP. The active form of *E. coli* RNR is thought to be a 1:1 mixture of α2 and β2, although there is only one Y$^\bullet$ per β2, suggesting the active RNR complex is asymmetric. One way to achieve complete inactivation of α2β2 with 1 F_2CDP is that once chemistry has occurred in the active site of the first α, it precludes chemistry from occurring in the active site of the second α. This chemistry further leads to a tight complex between the two subunits preventing recycling of the unmodified α. To test this model, the inactivation mixture and a number of controls (including one with a mixture of α, β, and ATP) were examined by using SEC on a Superose 12 FPLC column. All elution buffers contained either 0.5 mM ATP or 100 μM TTP previously shown to enhance α2 formation and more recently to enhance α2β2 interactions.

The results of SEC analysis of RNR inactivated with F_2CDP/ATP, with ATP in the elution buffer, are summarized in Fig. 2 *A–C* and Table 2. Fig. 2*A* reveals a single protein peak. Fractions collected through the protein peak were analyzed by scintillation counting and by SDS/PAGE. The former revealed 0.9 labels per α2β2 (Fig. 2*A*). The SDS/PAGE analysis (Fig. 2*B*) revealed the presence of α and β. Their relative ratios were determined in each fraction by comparison with standard curves made with known concentrations of α and β (Fig. 2*B*, standard curves not shown) and found to be ≈1:1 (Fig. 2*C*).

A control SEC analysis in the absence of F_2CDP, with ATP in the elution buffer reveals separation of α2 and β2 (Fig. 2 *D* and *E*). Analysis of the ratio of α:β supports this conclusion (Fig. 2*F*). The analysis in Fig. 2 suggests that a tight complex between subunits is unique to the presence of F_2CDP.

Further experiments were carried out to assess the resolution of the SEC method and to obtain information about the relative molecular masses of the observed protein peaks. The behavior of the individual subunits and complex were examined. In the absence of nucleotides, α migrates as a mixture of monomer and dimer with apparent molecular masses of 105 and 143 kDa (Table 2), respectively. The apparent molecular masses are obtained by comparison of the retention times of the eluting proteins with retention times of known molecular mass standards (SI Fig. 5). With ATP or TTP in the running buffer, α now migrates as a dimer (α2) of 174 kDa (Table 2 and SI Fig. 5). When RNR is inactivated by [1′-^{3}H] F_2CDP/ATP and chromatographed with ATP in the running buffer, the protein has an apparent molecular mass of 277 kDa (Fig. 2*A* and SI Fig. 5). The SEC analysis presented in Fig. 2 *A–C*, the stability of the complex during the inactivation reaction and the subsequent 25 min chromatogratography, and the apparent molecular mass suggests that the active form of RNR is α2β2 and that the interaction between the subunits has dramatically increased relative to the non-nucleotide bound forms (Table 2).

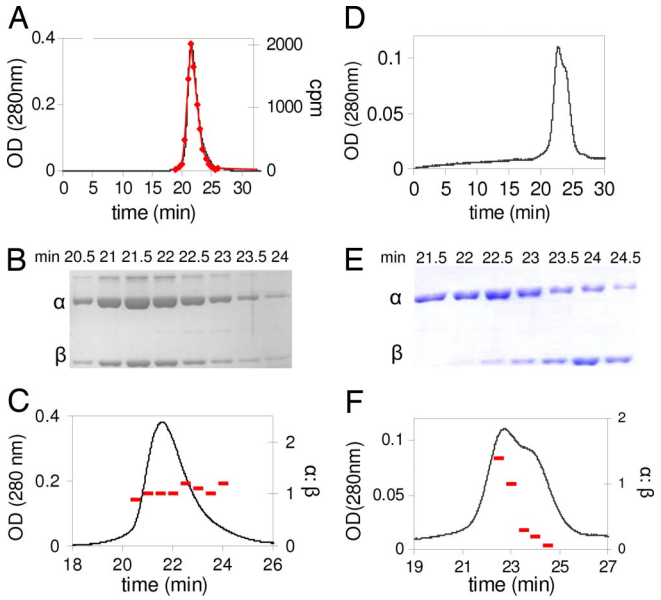

Fig. 2. SEC on a Superose 12 column to detect complex formation (α2β2) in *E. coli* RNR incubated with ATP in the presence or absence of [1′-^{3}H] F_2CDP. Elution buffer contains 0.5 mM ATP. (*A–C*) Presence of F_2CDP. (*A*) Elution profile monitored by $A_{280\ nm}$ and scintillation counting (♦). (*B*) Fractions through the protein peak in A monitored by SDS/PAGE. Note the slower migrating band (5% of the protein) is an altered conformation of α. (*C*) Analysis of the ratio of α:β (−), using standard curves generated from known amounts of α and β. (*D–F*) Absence of F_2CDP. (*D*) Elution profile. (*E*) Fractions through the protein peak in *D* monitored by SDS/PAGE. (*F*) Analysis of the ratio of α:β, using standard curves generated from known amounts of α and β.

Subunit Interactions of Human RNR in the Presence of F_2CDP. A similar set of experiments has been carried out with the human RNR. The Cooperman laboratory has demonstrated that in contrast with the prokaryotic RNRs, the active mouse RNR can be α2β2, α6β2, and α6β6 depending on the concentration of ATP (18). Recent studies using gas phase electrophoretic mobility macromolecule analysis have suggested that the active form of hRNR is α6β2 (24). Biacore studies and kinetic studies demonstrate that the interactions between α and β in the absence of nucleotides, as in the prokaryotic case, are weak (K_d = 0.2 μM) (21). Anticipated differences in the aggregation state of active RNR relative to the *E. coli* RNR caused us to switch to a Superdex 200 column for molecular mass analysis in the presence and absence of F_2CDP in addition to ATP. The results of incubation of either 0.5 or 1 eq of [1′-^{3}H] F_2CDP/ATP by SEC with ATP in the elution buffer are shown in Fig. 3 *A* and *B* and are summarized in Table 2. Fractions were collected through the protein peak and analyzed by scintillation counting and by SDS/PAGE (Fig. 3*B*). In the former case, analysis gave 0.8 radiolabels/α2. SDS/PAGE revealed the presence of both α and β. The relative ratio of α:β of 1:1 was established by using standard curves made from α and β (SI Fig. 6).

Experiments were also carried out to assess the resolution of the SEC method and to obtain information about the relative molecular masses of the observed protein peaks. β2 migrates with an apparent molecular mass of 108 kDa (calculated 94.1 kDa; SI Fig. 7). α in the absence of nucleotides migrates as the expected monomer, whereas in the presence of TTP, it migrates as a dimer of 189 kDa (SI Fig. 7). The retention time of the protein peak eluted from the RNR inactivated with F_2CDP/ATP and with ATP in the elution buffer, relative to molecular mass standards reveals an apparent molecular mass of 872 kDa (SI Fig. 7). The 1:1 ratio of α:β, the radiolabeling of the complex, and the apparent molecular mass in comparison with the expected mass of 834 kDa for α6β6, 646 kDa for α6β2, and 278 kDa for α2β2, suggest that the active form of the

Table 2. Molecular mass determination of *E. coli* and human RNR and their subunits by SEC

Protein	Protein (effector)	Apparent mass, kDa	Expected mass, kDa	Oligomeric state
E. coli RNR	β	96	87	$\beta 2$
	α*	143, 105	172, 86	$\alpha 2$, α
	α (100 μM TTP)	174	172	$\alpha 2$
	α (0.5 mM ATP)	174	172	$\alpha 2$
	α, β*	156, 108	172, 87	$\alpha 2$, $\beta 2$
	α, β (ATP)†	167, 109	172, 87	$\alpha 2$, $\beta 2$
	α, β inactivated by F_2CDP†	277	259	$\alpha 2\beta 2$ complex
Human RNR	β	108	94	$\beta 2$
	α	88	92	α
	α (100 μM TTP)	189	184	$\alpha 2$
	α, β (ATP)	589, 94	553, 94	$\alpha 6$, $\beta 2$
	α, β inactivated by F_2CDP†‡	872	834	$\alpha 6\beta 6$ complex

*The HPLC trace indicates multiple species. Gaussian fits to the peak shape, using Origin software, Version 6.1, gave the peak retention times.

†Elution buffer contains 0.5 mM ATP. Fractions were collected through the protein peak and were analyzed by 10% SDS/PAGE as summarized in Fig. 2 *A–F* and Fig. 3.

‡Peak I, apparent mass 872 kDa ($\alpha 6\beta 6$, 834 kDa) based on standard curve (SI Fig. 6); Peak II: ArnA, apparent mass 484 kDa (hexamer of ArnA is 446 kDa); Peak III, subunit molecular mass 65 kDa based on SDS/PAGE.

human RNR is $\alpha 6\beta 6$ and that the subunits are tightly interacting. The results, as in the case of the *E. coli* RNR, provide an explanation for complete RNR inactivation with substoichiometric amounts of F_2CDP. Inactivation of class I RNRs by F_2CDP thus provides another paradigm for inhibitor design of this protein: increasing the subunit affinity.

A number of additional features in the chromatogram in Fig. 3*A*, peaks II and III, require comment. Two proteins copurify with α and can be seen on SDS/PAGE with subunit molecular masses of 74 kDa and 65 kDa. The protein from peak II was isolated, sequenced and identified as an *E. coli* protein Arna, which exists as a hexamer in its native state (33). The identity of peak III has not been determined, but SDS/PAGE analysis reveals it is not associated with RNR. Efforts to further purify α via peptide and dATP affinity chromatography and several different anion exchange methods failed, because α is not very soluble and is prone to aggregation. Recovery of α and radiolabel from the column was 82%. The difference in the intensity of proteins in peak II and III (Fig. 3*A*) relative to SDS/PAGE is not understood.

Discussion

Many 2′-substituted-2′-deoxynucleotides have been shown to be potent mechanism based inhibitors of RNRs because the initial experiments in 1976 (34). Detailed studies on 2′-fluoro, 2′-chloro and 2′-azido derivatives have provided the basis for a general mechanism of inhibition by these substrate analogs (Scheme 1) (35, 36). The $Y^{\bullet}$ in β is reduced and generates a transient thiyl radical

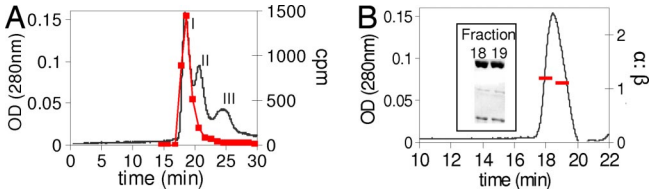

Fig. 3. SEC on a Superdex 200 column to detect the complex formation (αnβn) in human RNR upon inactivation by F_2CDP/ATP. (*A*) The elution profile monitored by A_{214} and scintillation counting (■). (*B*) Fractions through the protein peak in *A* monitored by SDS/PAGE and analysis of the ratio of α:β using standard curves generated from known amounts of α and β. Peak I contains α and β; Peak II contains Arna; and Peak III contains no α or β, but an unidentified protein of monomer molecular mass 65 kDa. We have repeated this experiment with homogeneous α (provided by the C. G. Dealwis laboratory, University of Tennessee, Knoxville, TN). The results are identical, but look cleaner, because the *E. coli* contaminating protein has been removed.

in α that initiates nucleotide reduction by 3′-hydrogen atom abstraction. Loss of the 2′ substituent (HO^-, F^-, Cl^-, N_3^-, or their conjugate acids) results in formation of intermediate A, which then partitions into two pathways depending on whether the 2′-radical is reduced by the top face thiol or a bottom face thiol. In the former case, the inactivation is caused by formation of a 3′-ketodeoxynucleotide which dissociates from the active site and decomposes to generate the nucleic acid base, pyrophosphate, and a furanone. The furanone then alkylates α resulting in its inactivation. In the case of bottom face reduction, in addition to generating the 3′-ketodeoxynucleotide that eventually inactivates α from solution through the furanone, the $Y^{\bullet}$ in β remains reduced, thus β also becomes inactivated. Most 2′-substituted deoxynucleotides inhibit class I RNRs by a combination of these pathways.

Studies presented herein suggest an additional mechanism by which 2′-substituted nucleotides may inactivate RNR. Gemzar has two fluorines at C2′. Both are lost during inactivation, at least in the case of the *E. coli* and *Lactobacillus leichmannii* RNRs, which have thus far been examined (12, 13). In addition, with [1′-^{3}H] F_2CDP inactivation is accompanied by 0.5 eq of sugar labeling from F_2C/α, ≈20–40% of tyrosyl radical loss and 100% loss of RNR activity. The mechanisms by which F_2CDP inactivate the *E. coli* and human RNRs, thus, must occur by multiple pathways as previously observed with other 2′-substituted nucleotides. Furthermore, all pathways result in covalent labeling with the sugar of F_2CDP and loss of cytosine. The details of the inactivation mechanism are complex and are not yet understood.

The observation of substoichiometric amounts of nucleotide resulting in complete RNR inactivation, at face value, seems difficult to understand. An explanation for the unusual stoichiometry is provided by the analysis of the RNR quaternary structure. In the case of the *E. coli* RNR, SEC reveals a tight $\alpha 2\beta 2$ complex (Fig. 2 *A–C*) when it is inactivated by F_2CDP. A control in the absence of F_2CDP reveals that $\alpha 2$ separates from $\beta 2$ by the same chromatographic analysis (Fig. 2 *D–F*). In retrospect, we have previously seen this type of behavior with another substoichiometric mechanism based inhibitor: 2′-azido-2′-deoxynucleotides, N_3NDP (19, 37, 38). During a 2-min incubation of RNR with [5′-^{3}H] N_3NDPs, >90% of RNR activity is lost, 50% of $Y^{\bullet}$ is lost, and 0.7 eq radiolabel are associated with RNR. Protein denaturation, however, resulted in radiolabel release suggesting it is noncovalently bound or covalently bound in an unstable structure. In contrast with F_2CDP, activity of α with N_3UDP is recovered to 50% and complete inactivation over 30 min is associated with 100% loss of $Y^{\bullet}$. Thus, although the subunits must be tightly associated initially to account for >90% loss of activity with just 50% loss of

$Y^{\bullet}$, further chemistry associated with nucleotide allows subunit weakening and dissociation. An SEC experiment similar to the one described in Fig. 2 provides no evidence for an $\alpha 2\beta 2$ complex (SI Fig. 8). The unique chemistry associated with the different inhibitors thus can dramatically effect subunit interactions.

Inactivation of the human RNR, at least in the presence of reductant, mirrors the observations made with the *E. coli* RNR. One major difference, however, involves the quaternary structure of the human RNR. Our SEC studies have provided direct evidence in support of an active $\alpha 6\beta 6$ complex. This result contrasts with previous proposals of active $\alpha 2\beta 2$ and with the recent mass spectrometric studies suggesting that $\alpha 6\beta 2$ is the active form of RNR (24). Our results support the importance of the $\alpha 6$ form of the large subunit, first proposed by Cooperman's laboratory (18). The SEC results also suggest that inactivation is the result of tight complex formation between the subunits that can occur even in the presence of substoichiometric amounts of nucleotide. At odds with this interpretation are the activity assays for each subunit in the presence of an excess of the second subunit. If a tight complex were present subsequent to inactivation, one would have expected that α and β would be 100% inactive. Although this was the case for α (SI Fig. 4), $\beta 2$ retains 60% of its activity. These results are very intriguing and provide us with additional insight about subunit interaction. The recovery of $\beta 2$ activity requires that excess α can form a transient ternary complex with $\alpha 6\beta 6$ and liberate $\beta 2$, which has retained some of its $Y^{\bullet}$ and is thus active. This proposal is supported by a recent structure of a complex of the $\alpha 2\beta 2$ from *E. coli* where only one of the two βs interacts with α (39). Thus, one could propose that binding of α to the unattached β of $\beta 2$ could facilitate $\alpha 2$ release. In the case of the inactivated $\alpha\alpha^{*}\beta 2$ complex assayed with excess α (α^{*} = covalently labeled α), this mechanism would result in release of $\alpha\alpha^{*}$ and formation of active $\alpha 2\beta 2$. Because there is only one [^{3}H]-label per $\alpha 2$, one would have expected the unlabeled monomer to be also active in the presence of excess β, but this is not the case. Thus, this result provides strong support for asymmetry within the $\alpha 2$ ($\alpha 6$); that is, modification of one α precludes activity of the other. The results suggest that if the cell was able to increase the amount of α, then active RNR could be recovered. Interestingly resistance in a number of cell lines has identified elevated α levels (40–42). F_2CDP is unique with respect to the well characterized 2′-substituted nucleotide mechanism based inhibitors, in that in addition to labeling α and loss of $Y^{\bullet}$ on β, inactivation is the result of tight subunit association.

Summary. RNR is inactivated by 0.5 eq of F_2CDP/α, as a consequence of altering the affinity of its two subunits and generating an asymmetric interaction within this complex. Recent studies using α and β substituted site specifically with unnatural amino acids have also been interpreted to suggest an asymmetry within the active RNR complex (19, 20). Our results suggest that the paradigm of a 1:1 symmetrical complex between the two subunits of RNR must be re-evaluated. They further suggest a novel mode of inactivation of RNR.

Materials and Methods

[5-^{3}H] F_2C and 2-deoxy-3,5-di-*O*-benzoyl-3,3-difluororibonolactone were kind gifts of Eli Lilly (Indianapolis, IN). Competent *E. coli* BL 21 (DE3) cells were purchased from Stratagene (La Jolla, CA). Complete EDTA-free protease inhibitor tablets and calf alkaline phosphatase (20 units/μl) were purchased from Roche Biochemicals (Indianapolis, IN). Plasmids containing the genes for α (formerly called H1) and β (formerly called H2), phRRM1, and phRRM2, were generous gifts from Y. Yen (City of Hope National Medical Center). Protein concentrations were determined by using extinction coefficients ($\varepsilon_{280\ nm}$) per monomer [45,900 M^{-1} cm^{-1} for $(His)_6$-β and 119,160 M^{-1} cm^{-1} for α]. *E. coli* TR (specific activity of 40 units/mg) and TR reductase (specific activity of 1,320 units/mg) were isolated as described in refs. 43 and 44.

Expression Plasmids for Human α and β in *E. coli*. Sequencing of the α and β genes in phRRM1 and phRRM2, respectively, revealed a number of mutations relative to the sequences reported in the NCBI database (27, 28). In the α gene, nucleotide C521 was mutated to a T, resulting in a Val to Ala substitution. At residue 1763, C was changed to T, resulting in an Ile to Thr substitution. In the gene for β, A650 was changed to G, resulting in the conversion of a Lys to Arg. These mutations were corrected by site-directed mutagenesis, using the QuikChange Kit by Stratagene. In addition the N-terminal tags of each protein were reengineered to minimize the number of additional residues. The NdeI digestion site in α was silenced. Both α and β genes were digested with NdeI and NotI and ligated into the NdeI–NotI sites of pET-28a (Novagen) to produce $(His)_6$-α and $(His)_6$-β containing a MGSSHHHHHHS-SGLVPRGSH-N terminus. All constructs were verified by sequencing at the MIT biopolymers laboratory.

Expression and Purification of Human α and β. phRRM1 and phRRM2 were transformed into *E. coli* BL21 (DE3) (Stratagene) and plated on LB agar plates with 50 μg/ml kanamycin, and a single colony was chosen for growth. For isolation of β, an overnight culture (40 ml) grown to saturation was diluted into 2 liters of LB containing 50 μg/ml kanamycin and grown at 37°C to an OD_{600} of 0.7–0.9. Isopropyl-1-thio-β-D-galactopyranoside (1 mM) was then added, and the cells were grown for an additional 6 h at 30°C. For growth of α, an overnight culture (40 ml) was grown from a single colony at 37°C and transferred to 2 liters of LB and grown at 37°C. Isopropyl-1-thio-β-D-galactopyranoside (1 mM) was added at an OD_{600} of 0.7–0.9, and the cells were grown overnight at 25°C. The isolation of $\beta 2$ and α were carried out by the following general procedure: The cells were harvested and typically yielded 4 g/liter. The cell pellets were suspended (5 vol/g) in 50 mM NaH_2PO_4, pH 7.0, 0.1% Triton X-100, and 10 mM 2-mercaptoethanol. The suspension was passed through the French press at 14,000 psi. The cell lysate was centrifuged at 20,000 $\times$ *g* for 30 min. The supernatant was treated with streptomycin sulfate to a final concentration of 1% (wt/vol), and the pellet was removed by centrifugation. The supernatant was incubated with Ni-NTA agarose resin (1 ml/g of cells; Qiagen, Valencia, CA) at 4°C for 1 h and then loaded into a column (2.5 $\times$ 10 cm). The column was subsequently washed with 40 column vol of 50 mM NaH_2PO_4/800 mM NaCl/50 mM imidazole, pH 7.0/0.1% Triton X-100/10 mM 2-mercaptoethanol. The protein was eluted with 50 mM NaH_2PO_4/300 mM NaCl/125 mM imidazole, pH 7.0. Fractions containing protein were identified by using the Bradford assay. The fractions were pooled and concentrated to $<$10 ml, and then the imidazole was removed by Sephadex G-25 chromatography (200 ml, 2.5 $\times$ 50 cm). $\beta 2$ was stored in 50 mM Tris, 100 mM KCl, pH 7.6, 5% glycerol. α was stored in 50 mM Tris, 100 mM KCl, 15 mM $MgCl_2$, 5 mM DTT, pH 7.6, 5% glycerol. Protein yields of α and β were $\approx$2 mg and 15 mg/liter culture, respectively. The purity of α and β were analyzed on 10% SDS/PAGE. Two more rapidly migrating bands detected by SDS/PAGE copurified with α. One of these impurities, identified by sequencing, is Arna, a hexameric *E. coli* protein with a subunit molecular mass of 74 kDa. The second impurity has not been identified.

Conversion of Human apo $\beta 2$ to Holo $\beta 2$. Stock solutions of $(His)_6$-$\beta 2$ (2 ml, 2.5 mg/ml) were deoxygenated by 6 cycles of evacuation (for 3 $\times$ 10 s) followed by argon flushing (2 min) on a Schlenk line. The deoxygenated $\beta 2$ solution was brought into the glovebox (MBraun, Stratham, NH) and 5 eq of Fe(II) per $\beta 2$ was added from a $FeNH_4SO_4$ solution in buffer A (50 mM Tris/100 mM KCl, pH 7.6/5% glycerol). The resulting mixture was incubated at 4°C for 15 min. The protein was then removed from the glovebox, and 1 ml of O_2 saturated buffer A (50 mM Tris/100 mM KCl, pH 7.6, 5%) was added. Excess iron was removed by Sephadex G-25 chromatography (40 ml, 2.5 $\times$ 20 cm).

Activity Assays. A reaction mixture contained, in a final volume of 350 μl, 50 mM Hepes (pH 7.6), 15 mM $MgCl_2$, 1 mM EDTA, 0.3 μM (or 2.1 μM) α, 2.1 μM (or 0.3 μM) β, 3 mM ATP, 1 mM [^{3}H]-CDP (specific activity 3,400 cpm/nmol), 100 μM *E. coli* TR, 1.0 μM TR reductase, and 2 mM NADPH. The assay mixture was preincubated at 37°C for 3 min, and the reaction was initiated by the addition of CDP. Aliquots (50 μl) were removed over a 15-min time period and quenched in a boiling water bath. dCDP production was analyzed by the method of Steeper and Steuart (45).

Time-Dependent Inactivation Studies. The inactivation mixture contained in a final volume of 100 μl: 1.2 μM α/1.2 μM β/3 mM ATP/1 mM [^{3}H]-CDP (specific activity 3,400 cpm/nmol)/5 mM DTT/50 mM Hepes (pH 7.6)/15 mM $MgCl_2$/1 mM EDTA. The reaction was initiated by addition of F_2CDP (0.6 μM, 1.2 μM and 6 μM, final concentrations) and incubated at 37°C. Aliquots (12.5 μl) were removed from 30 s to 17 min and assayed for dCDP production as described above. Control experiments were carried out in which the F_2CDP was omitted.

Quantitation of Covalent Labeling of *E. coli* RNR and Human RNR with [1′-^{3}H]-F_2CDP and [5-^{3}H]-F_2CDP. A typical reaction mixture (5.5 μM α, β in 300 μl) was identical to that described above, except that F_2CDP was replaced by either [1′-^{3}H]-F_2CDP (5,889 cpm/nmol) or [5-^{3}H]-F_2CDP (6,643 cpm/nmol). After 10 min at 37°C, a 270-μl aliquot was loaded onto a Sephadex G-50 column (1 × 20 cm, 20 ml) that was preequilibrated with the assay buffer (50 mM Hepes/15 mM $MgCl_2$/1 mM EDTA, pH7.6) or made 6 M in guanidine·HCl and loaded onto a Sephadex G-50 column with assay buffer containing 2 M guanidine·HCl. Fractions (1 ml) were collected and assayed for A_{280} and A_{260}, and 500 μl of each fraction was analyzed by scintillation counting.

Quantification of Cytosine Released During the Inactivation of *E. coli* and Human RNR by [5-^{3}H]-F_2CDP. The reaction mixture was as described in *Time-Dependent Inactivation Studies* (1.2 μM human RNR α, β in 500 μl). The reaction was initiated by addition of 1.2 μM [5-^{3}H]-F_2CDP (6643 cpm/nmol). After 20 min, the inactivation mixture was filtered through an YM-30 Centricon device (Millipore, Billerica, MA) at 4°C. F_2C (120 nmol) and cytosine (120 nmol) were added as carriers before filtration. The flow-through was treated with 30 units of alkaline phosphatase (Roche) for 3 h at 37°C and filtered through a second YM-30 Centricon device. The flow through was analyzed by using a Waters (Milford, MA) 2480 HPLC with an Altech Adsorbosphere Nucleotide Nucleoside C-18 column (250 mm × 4.6 mm) at a flow rate of 1 ml/min. The elution buffer contained buffer A (10 mM NH_4OAc, pH 6.8) and buffer B (100% methanol). A 10-min isocratic elution was followed by a linear gradient to 40% B over 30 min. A linear gradient was then run to 100% B over 5 min. Fractions (1 ml) were collected, and 200 μl of each were analyzed by scintillation counting. Standards were as follows: retention times are: cytosine, 5.7 min; cytidine, 12.6 min; *ara*-C, 17.4 min; dC, 19.0 min and F_2C, 23.2 min. The recovery of cytosine and F_2C was calculated based on the UV spectrum (cytosine, λ_{267}, $\varepsilon = 6100\ M^{-1}\ cm^{-1}$, F_2C, λ_{268}, $\varepsilon = 9360\ M^{-1}\ cm^{-1}$). The radioactivity recovered with cytosine and F_2C was analyzed by scintillation counting.

SEC to Examine the Quaternary Structure of RNRs Subsequent to Inactivation by F_2CDP. SEC was performed by using a Superose 12 column (10 × 300 mm, GE Healthcare, Little Chalfont, U.K.) for *E. coli* RNR or a Superdex 200 column (10 × 300 mm, GE Healthcare) for human RNR attached to a Waters 2480 HPLC. Gel filtration molecular mass standards (GE Healthcare) were ovalbumin, 43 kDa; conalbumin, 75 kDa; aldolase, 158 kDa; pyruvate kinase, 232 kDa or catalase 232 kDa; ferritin, 440 kDa; thyroglobulin, 669 kDa; and blue dextran, 2,000 kDa. The elution buffer was 50 mM Hepes (pH 7.6)/15 mM $MgCl_2$/0.5 mM ATP, with or without 150 mM KCl. Molecular mass standards were run at the beginning of each experiment. The reaction mixture was prepared as described above (15 μM α, β in 300 μl or 30 μM α, β in 150 μl). After 10 min of incubation, 150 μl or 300 μl was injected onto the column. The elution rate was 0.5 ml/min and 0.5 ml fractions were collected. If [1′-^{3}H]-F_2CDP was used in the inactivation, 100-μl aliquots of each fraction was analyzed by scintillation counting.

Quantitative Analysis of the Subunits of *E. coli* and Human RNRs by SDS/PAGE. The fractions collected from the SEC analysis were analyzed by 10% SDS/PAGE and compared with concentrations of α and β from *E.coli* RNR (0.4 μM to 3.2 μM) or human RNR (0.2 μM to 1.6 μM) as standards. The proteins were visualized with Coomassie blue staining. The band intensities were quantified by using Quantity One software (Bio-Rad, Hercules, CA). The concentrations of α and β in the complex were determined from the standard curves.

We thank Dr. Yun Yen for providing phRRM1 and phRRM2 plasmids, Eli Lilly for providing F_2C, the Chris G. Dealwis group laboratory for supplying us with homogeneous α. This work was supported by National Institutes of Health Grant GM 29595 and David Koch funds from The Massachusetts Institute of Technology Center for Cancer Research.

1. Hertel LW, Boder GB, Kroin JS, Rinzel SM, Poore GA, Todd GC, Grindey GB (1990) *Cancer Res* 50:4417–4422.
2. Huang P, Chubb S, Hertel LW, Grindey GB, Plunkett W (1991) *Cancer Res* 51:6110–6117.
3. Plunkett W, Huang P, Gandhi V (1997) *Nucleosides Nucleotides* 16:1261–1270.
4. Mackey JR, Mani RS, Selner M, Mowles D, Young JD, Belt JA, Crawford CR, Cass CE (1998) *Cancer Res* 58:4349–4357.
5. Bergman AM, Pinedo HM, Peters GJ (2002) *Drug Resist Updat* 5:19–33.
6. Garcia-Manteiga J, Molina-Arcas M, Casado FJ, Mazo A, Pastor-Anglada M (2003) *Clin Cancer Res* 9:5000–5008.
7. Usova EV, Eriksson S (1997) *Eur J Biochem* 248:762–766.
8. Van Rompay AR, Johansson M, Karlsson A (1999) *Mol Pharmacol* 56:562–569.
9. Lohman GJS (2006) PhD Thesis (MIT, Cambridge, MA).
10. Heinemann V, Xu YZ, Chubb S, Sen A, Hertel LW, Grindey GB, Plunkett W (1990) *Mol Pharmacol* 38:567–572.
11. Baker CH, Banzon J, Bollinger JM, Stubbe J, Samano V, Robins MJ, Lippert B, Jarvi E, Resvick R (1991) *J Med Chem* 34:1879–1884.
12. van der Donk WA, Yu GX, Perez L, Sanchez RJ, Stubbe J, Samano V, Robins MJ (1998) *Biochemistry* 37:6419–6426.
13. Silva DJ, Stubbe J, Samano V, Robins MJ (1998) *Biochemistry* 37:5528–5535.
14. Gandhi V, Legha J, Chen F, Hertel LW, Plunkett W (1996) *Cancer Res* 56:4453–4459.
15. Miura S, Izuta S (2004) *Curr Drug Targets* 5:191–195.
16. Nordlund N, Reichard P (2006) *Annu Rev Biochem* 75:681–706.
17. Kolberg M, Strand KR, Graff P, Andersson KK (2004) *Biochim Biophys Acta* 1699:1–34.
18. Kashlan OB, Scott CP, Lear JD, Cooperman BS (2002) *Biochemistry* 41:462–474.
19. Fritscher J, Artin E, Wnuk S, Bar G, Robblee JH, Kacprzak S, Kaupp M, Griffin RG, Bennati M, Stubbe J (2005) *J Am Chem Soc* 127:7729–7738.
20. Seyedsayamdost MR, Stubbe J (2006) *J Am Chem Soc* 128:2522–2523.
21. Ingemarson R, Thelander L (1996) *Biochemistry* 35:8603–8609.
22. Thelande L (1973) *J Biol Chem* 248:4591–4601.
23. Brown NC, Reichard P (1969) *J Mol Biol* 46:39–55.
24. Rofougaran R, Vodnala M, Hofer A (2006) *J Biol Chem* 281:27705–27711.
25. Kohn P, Samaritano RH, Lerner LM (1965) *J Am Chem Soc* 87:5475–5480.
26. Chou TS, Heath PC, Patterson LE, Poteet LM, Lakin RE, Hunt AH (1992) *Synthesis* 565–570.
27. Parker NJ, Begley CG, Fox RM (1991) *Nucleic Acids Res* 19:3741.
28. Pavloff N, Rivard D, Masson S, Shen, SH., MesMasson AM (1992) *DNA Sequence* 2:227–234.
29. Bollinger JM, Tong WH, Ravi N, Huynh BH, Edmondson DE, Stubbe J (1995) *Methods Enzymol* 258:8–303.
30. Guittet O, Hakansson P, Voevodskaya N, Fridd S, Graslund A, Arakawa H, Nakamura Y, Thelander L (2001) *J Biol Chem* 276:40647–40651.
31. Shao JM, Zhou BS, Zhu LJ, Qiu WH, Yuan YC, Xi BX, Yen Y (2004) *Cancer Res* 64:1–6.
32. Ortigosa AD, Hristova D, Perlstein DL, Zhang Z, Huang MX, Stubbe J (2006) *Biochemistry* 45:12282–12294.
33. Gatzeva-Topalova PZ, May AP, Sousa MC (2005) *Structure (London)* 13:929–942.
34. Thelander L, Larsson B (1976) *J Biol Chem* 251:1398–1405.
35. Licht S, Stubbe J (1999) in *Mechanistic Investigations of Ribonucleotide Reductases*, ed Poulter CD (Elsevier, Amsterdam), pp 163–203.
36. Stubbe JA, van der Donk WA (1995) *Chem Biol* 2:793–801.
37. Salowe S, Bollinger JM, Ator M, Stubbe J, McCracken J, Peisach J, Samano MC, Robins MJ (1993) *Biochemistry* 32:12749–12760.
38. Salowe SP, Ator MA, Stubbe J (1987) *Biochemistry* 26:3408–3416.
39. Uppsten M, Färnegårdh M, Domkin V, Uhlin U (2006) *J Mol Biol* 359:365–377.
40. Davidson JD, Ma LD, Flagella M, Geeganage S, Gelbert LM, Slapak CA (2004) *Cancer Res* 64:3761–3766.
41. Bergman AM, Eijk PP, van Haperen V, Smid K, Veerman G, Hubeek I, van den Ijssel P, Ylstra B, Peters GJ (2005) *Cancer Res* 65:9510–9516.
42. Jordheim LP, G. O., Lepoivre M, Galmarini CM, Dumontet C (2005) *Mol Cancer Ther* 4:1268–1276.
43. Russel M, Model P (1985) *J Bacteriol* 163:238–242.
44. Lunn CA, Kathju S, Wallace BJ, Kushner SR, Pigiet V (1984) *J Biol Chem* 259:469–474.
45. Steeper JR, Steuart CC (1970) *Anal Biochem* 34:123–130.